NANO LETTERS

2004
Vol. 4, No. 1
85−88

Enhanced Absorption Induced by a Metallic Nanoshell

Roi Baer*

Department of Physical Chemistry and the Lise Meitner Center for Quantum Chemistry, The Hebrew University of Jerusalem, Jerusalem 91904 Israel

Daniel Neuhauser and Shimon Weiss

Department of Chemistry and Biochemistry, University of California, Los Angeles, California 90095-1569

Received October 16, 2003; Revised Manuscript Received November 14, 2003

ABSTRACT

Nanoshells have been previously shown to have tunable absorption frequencies that are dependent on the ratio of their inner and outer radii. Inspired by this, we ask: can a nanoshell increase the absorption of a small core system embedded within it? A theoretical model is constructed to answer this question. A core, composed of a "jellium" ball of the density of gold is embedded within a jellium nanoshell of nanometric diameter. The shell plasmon frequency is tuned to the core absorption line. A calculation based the time-dependent density functional theory was performed showing a 10 fold increase in core excitation yield.

I. Introduction. The development of photonic probes of sufficient absorption and/or emission is an important problem in nanomaterials and nanobiotechnology research. Typically, for biological and biomedical applications, one is interested in the development of nanoscale probes for imaging and therapeutic purposes.[1] However, these have, by the nature of their size, a small absorption cross-section compared with bulk (large) materials. Although the oscillator strength is in principle proportional to the volume of the absorbing particle,[2] and therefore large absorption could not be expected for a very small particle, it is conceivable that nanostructuring of materials coupled with band gap/molecular orbital engineering could considerably enhance the absorption of a nanoparticle at particular regions of the electromagnetic spectrum. The manipulation of structure and composition on the nanoscale could offer interesting possibilities. For example, strong electronic transitions of dye molecules or semiconductor nanocrystals could be coupled to plasmon resonances in small metallic particles. Such an enhancement could be very useful in also increasing the cross-section for emission of fluorescing nanoparticles or increasing heat delivery and photoablation for therapeutic purposes.[1,3] The main motivation is the increase of absorption cross-section while maintaining smallest size particles possible (to penetrate crowded environments such as the biological milieu of the live tissue).

For typical metals, however, the coupling is problematic. The bulk plasmon resonance of metals is at high frequencies (typically excitation energies of 5 eV), compared with 1−2 eV electronic transitions of molecules/semiconductors in the visible range. In recent years, experimental and theoretical investigations on metals have revealed the applicability of nanoshells.[4,5] Nanoshells consist of a dielectric core surrounded by a metallic shell of nanometric thickness. The plasmon absorption frequencies range from the high bulk value down to zero, determined by the ratio of the inner and outer shell radii (lowered with smaller relative thickness). Westcott et al.[6] have experimentally constructed plasmon shells with controlled absorption frequency.

The shell frequency is tuned to match the optical properties of the absorbing core, leading to hybridization/mixing and possibly overall enhancement of absorption cross-section of the composite nanoparticle or its individual components.

Prodan et al.[5,7−9] have developed a method, based on the frequency-domain time-dependent (TD) local-density approximation (LDA) to study this system theoretically, exploiting spherical symmetry. The formalism we use is physically equivalent to their approach. We enjoy an advantage (not used in the present paper) that our calculations, being done in real-time, can treat additional effects, such as response to strong fields, and are not limited to spherical symmetry.

In this study we examine and verify this idea using a simple model system, a metallic shell coupled to a small absorbing metallic dot ("onion" of a metallic core embedded in a metallic shell, see Figure 1). While currently limited only to plasmon−plasmon interactions, we plan in the future to expand this approach to plasmon−electronic transition

10.1021/nl034902k CCC: $27.50
Published on Web 12/09/2003

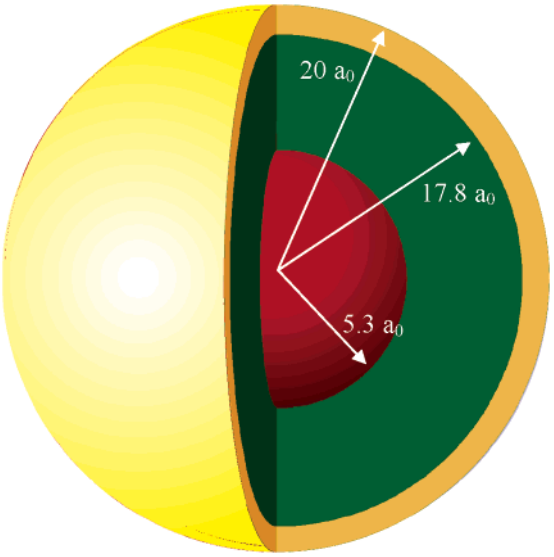

Figure 1. The core−shell model: the core is a "jellium" ball of uniform positive charge density surrounded by a thin shell of "jellium". Electrons are added such that the system is neutralized (not to scale).

coupling. The shell is significantly larger than the dot. We use time-dependent density functional theory, within the adiabatic local density approximation (ALDA) to study the system. This allows a reasonable description of the many-body effects. We show that a large mixing effect and enhancement of core absorption is indeed obtained.

Section II describes the theoretical method and calculations. Results are presented in section III, followed by conclusions in section IV.

II. The Model. The calculations are done in a TDDFT time-based plane-wave code. Specifically, we use a sparse grid on which we place a system made of two components, a shell and an inner core.

The shell has two radii; the outer radius is $R = 20$ a_0 and the inner radius is 17.8 a_0 (so the shell thickness is 2.2 a_0, a_0 is Bohr's radius). The shell is composed of uniform positive charge (jellium), of density $n_B = (4\pi r_s^3/3)^{-1}$ with $r_s = 3$ a_0 corresponding to the metallic density of gold. To avoid numerical difficulties associated with the Gibbs phenomena, the jellium density, $n_B(\mathbf{r})$, does not terminate abruptly at the shell edges but is instead smoothed out (the specific smoothing used here is with a Fermi−Dirac-like function with a width of 0.5 a_0).

The core is modeled as a ball of uniform charge (jellium) of the same density as the shell. The radius of the ball is small relative to that of the shell, $a = 5.32$ a_0. It is a well separated entity geometrically enclosed by the shell (we discuss this below in connection with Figure 2). The core plays the role of a small absorber, analogous to placing a molecule within the shell. Even though it has almost uniform density, its physics is different from that of the shell: the spectrum of the latter is dominated by strong plasmon response, while the small core shows several excitation lines reminiscent of single particle excitation spectra (Figure 3). No additional background potential was added to the system.

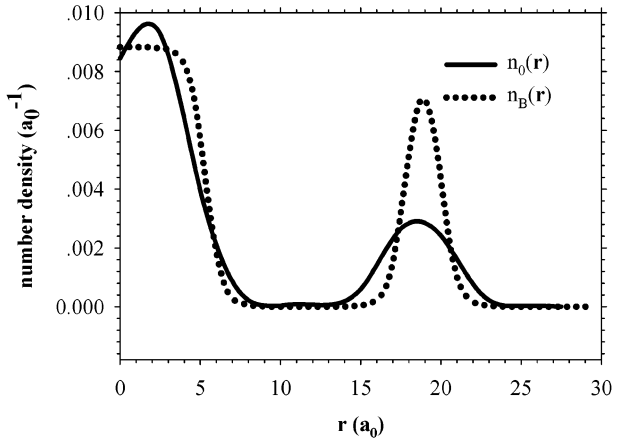

Figure 2. Radial profile of the positive ($n_B(\mathbf{r})$) and negative ($n_e(\mathbf{r})$) charge densities of the core−shell system. The core is a jellium ball of radius 5 a_0 and density given by $r_s = 3$ a_0.

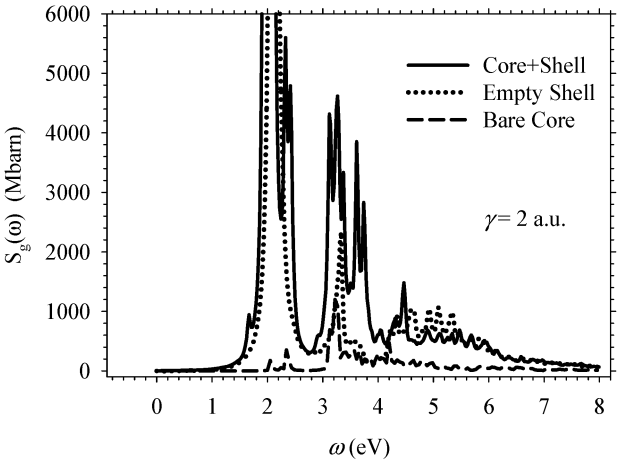

Figure 3. The dipole spectrum of the bare core, the empty shell and the core−shell systems.

The geometric size of the systems is chosen so that the total positive charge of the core is 6e (e is the absolute value of the electronic charge), while that of the shell is 88e. The number of electrons exactly neutralizes the system, $N_e = 94$ electrons. We minimize the Kohn−Sham energy functional with respect to $N_e/2$ one-electron orbitals

$$E_{KS}[\{\phi\}] = T_s\{\phi\} + E_{eN}[n] + E_H[n] + E_{LDA}[n] \quad (2.1)$$

where atomic units are used. Here $n(\mathbf{r}) = 2\sum_{j=1}^{N_e/2}\phi_j(\mathbf{r})^2$ is the electron density (the factor of 2 accounts for closed-shell spin effects), $T_s[\{\phi\}] = -\sum_{j=1}^{N_e/2}\langle\phi_j|\nabla^2|\phi_j\rangle$ is the independent-electron kinetic energy functional, $E_{eN}[n] = \int n(\mathbf{r})v_{eN}(\mathbf{r})\,d^3r$ is the electron-positive background interaction energy ($v_{eN}(\mathbf{r}) = -\int n_B(\mathbf{r}')/|\mathbf{r} - \mathbf{r}'|\,d^3r'$, where $n_B(\mathbf{r})$ is the positive background density), $E_H[n] = 1/2 \int\int n(\mathbf{r})n(\mathbf{r}')/|\mathbf{r} - \mathbf{r}'|\,d^3r\,d^3r'$ is the classical electron−electron repulsion energy, and finally, $E_{xc}[n]$ is the exchange correlation energy, within the local density approximation (LDA).[10] We minimize this energy functional, while keeping the orbitals ϕ_j orthonormal,[11] using the LDA Hamiltonian as a gradient:

$$\frac{\delta E_{KS}}{\delta \phi_j} = \hat{H}_{LDA}[n]\phi_j(\mathbf{r}) = -\frac{1}{2}\nabla^2\phi_j(\mathbf{r}) + v_s(\mathbf{r})\phi_j(\mathbf{r}) \quad (2.2)$$

where $v_s(\mathbf{r}) = v_{eN}(\mathbf{r}) + v_H(\mathbf{r}) + v_{LDA}(\mathbf{r})$, $v_H(\mathbf{r}) = \int n(\mathbf{r}')/|\mathbf{r} - \mathbf{r}'|\, d^3\mathbf{r}'$ is the Hartree potential, and $v_{LDA}(\mathbf{r}) = \delta E_{LDA}/\delta n(\mathbf{r})$ is the LDA exchange-correlation potential. Near cell electrostatic image effects are screened out.[12]

After determining the ground-state orbitals $\phi_j(\mathbf{r})$ and density $n_0(\mathbf{r})$, the absorption spectrum is computed using a linear response approach[13,14] based on TDDFT/adiabatic-LDA. The system is exposed to a short linearly polarized Gaussian "electric pulse" in the z direction $\eta E_z(t) = \eta E_0 \exp[-(t - t_c)^2/2\tau^2]$. The pulse is maximal at $t_c = 8$ a.u. and has a width $\tau = 2$ a.u. The term ηE_0 is a small electric field (η a small dimensionless linear-response factor). We use the fourth-order adaptive step-size Runge−Kutta algorithm to evolve the Kohn−Sham orbitals according to the equation[15]

$$i\dot{\psi}_j(\mathbf{r},t) = -\frac{1}{2}\nabla^2\psi_j(\mathbf{r},t) + v_s[n](\mathbf{r},t)\psi_j(\mathbf{r},t) \quad (2.3)$$

where $v_s(\mathbf{r},t) = v_{eN}(\mathbf{r}) + e\eta E(t)z + v_H(\mathbf{r},t) + v_{LDA}(\mathbf{r},t)$ and $\psi_j(\mathbf{r},t = 0) = \phi_j(\mathbf{r})$. The effective potential $v_s(\mathbf{r},t)$ is time dependent (TD) because it is affected by both the TD perturbation the TD density $n(\mathbf{r},t) = 2\sum_j|\psi_j(\mathbf{r},t)^2|$. Following the propagation for quite a long time (3000 a.u.) we Fourier transform the resulting dipole moment:

$$\mu(t) = \int z[n(\mathbf{r},t) - n_0(\mathbf{r},t)]\, d^3\mathbf{r} \quad (2.4)$$

obtaining the photoabsorption cross-section from:[2]

$$\Sigma_\gamma(\omega) \equiv \mathrm{Im}\frac{e\omega\tilde{\mu}(\omega)}{c\epsilon_0\sqrt{2\pi}\tau E_0 e^{i\omega t_c - \omega^2\tau^2/2}} \quad (2.5)$$

where $\tilde{\mu}(\omega) = \int_{-\infty}^{\infty}\mu(t)e^{i\omega t}e^{-\gamma t}\, dt$ is the frequency dependent dipole, c is the speed of light, and ϵ_o is the dielectric constant of vacuum. The parameter γ is a phenomenological decay parameter, representing a finite lifetime resulting from the interaction of the core−shell with the environment.

The frequency-dependent polarization includes a factor normalizing the density by the component of the perturbation at frequency ω. Also, n_0 is the density associated with propagating the orbitals in time but without the time-dependent perturbation $\eta V(\mathbf{r},t)$. Formally, if the initial orbitals converge to fulfill exactly the time-independent Kohn−Sham equations (eq 2.3) then n_0 would be the time-independent groundstate density, but this form for $\mu(t)$ helps circumvent any convergence errors.

It is straightforward to show that the resulting $\mu(\omega)$ is identical to the dipole moment which would have developed if a weak single-frequency perturbation would have been applied. It is an indication of the energy absorption by the system. Also, by Kubo's theorem[16] it is related to the commutator of the time-dependent and zero-time dipole moments (the so-called dipole−dipole correlation function).

The physical content of our TD linear-response approach is equivalent to the time-independent approaches applied extensively to nanoshells by Prodan and Nordlander.[5] The emphasis in our approach, however, is in the use here of a real-time method, or, more precisely, an iterative initial value problem so that no full inversion and diagonalization of the sizable Hamiltonian matrix is involved, and therefore a full 3D grid can be used without invoking symmetry. Interestingly, it is possible, as will be shown in an upcoming paper, to increase the efficiency of the method by avoiding the need to solve the nonlinear eq 2.3.

III. Results. The calculations were done on a 3-dimensional cubic grid of length $L = 60$ a_0, and uniform grid spacing of 2.5 a_0. This sparse grid spacing is sufficient since the potential wells of a jellium system are shallow, dictating small electronic kinetic energies.

Figure 2 shows the radial distribution of the positive background density $n_B(\mathbf{r})$ and the self-consistent field (SCF) electron density $n_0(\mathbf{r})$. The core and shell electron densities are well separated (in actual systems a dielectric material will be present in the shells). The total density is very similar to the sum of the two densities of the separated components. It therefore makes sense to speak about the core and shell as two separate entities, coupled by the electrostatic potential rather than any electron-sharing coupling. The electron density in the core is higher than in the shell, despite the fact that the positive charge densities are similar. This is due to the narrow spherical shell leading to a "spilled-over" electron density. The minimum Kohn−Sham potential, including the attractive background, the Hartree repulsion and the exchange correlation potentials, is −0.3 and −0.23 E_h in the core and shell, respectively. We have also computed the ionization potentials 4.7, 3.7, and 3.3 eV for the core, the shell, and core−shell, respectively.

The sum of the two separate system densities is to a high degree of accuracy equal to the density of the combined system. This is an indication of the weak initial coupling.

Figure 3 shows the photoabsorption cross section of the bare core, the empty shell, and the core−shell systems. An extremely strong absorption is seen for the shell and core shell at 2.1 eV, the plasmon frequency (the absorption cross section reaches 50 000 Mbarns). The core, too, has a peak at the same frequency; however, it is weaker by a factor of ∼300. The plasmon frequency of the shell is in fair agreement with calculated by Prodan and Nordlander.[5] The presence of the core considerably affects the absorption cross sections away from the plasmon resonance.

We should like to determine the degree of core excitation when it is surrounded by the shell. While a more complete calculation should concentrate on emission effects, in this letter we will use a simpler approach and consider absolute value of the core absorption function $|\Sigma_\gamma^{core}|$ obtained by plugging into eq 2.5 the "core dipole moment":

$$\mu_{core}(t) = \int_{|\mathbf{r}|<r_M} z[n(\mathbf{r},t) - n_0(\mathbf{r},t)]\, d^3\mathbf{r} \quad (2.6)$$

in place of the *total* dipole moment. Here r_M is a dividing radius, taken to be $r_M = 11$ a_0, (see Figure 2).

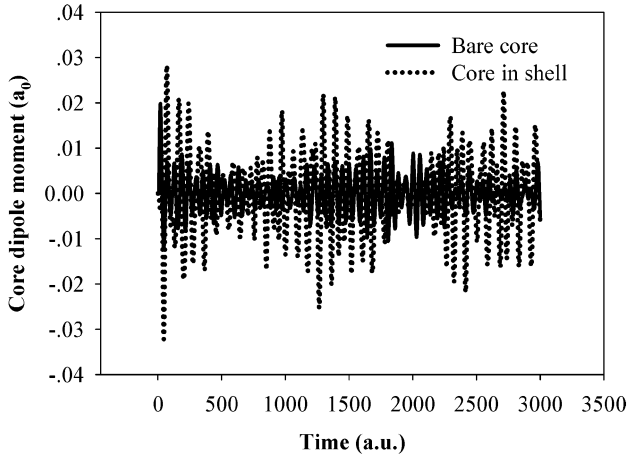

Figure 4. Time-dependent dipole of a bare and shell-enclosed core. The field strength is $10^{-4}\ E_h\ a_0^{-1}$.

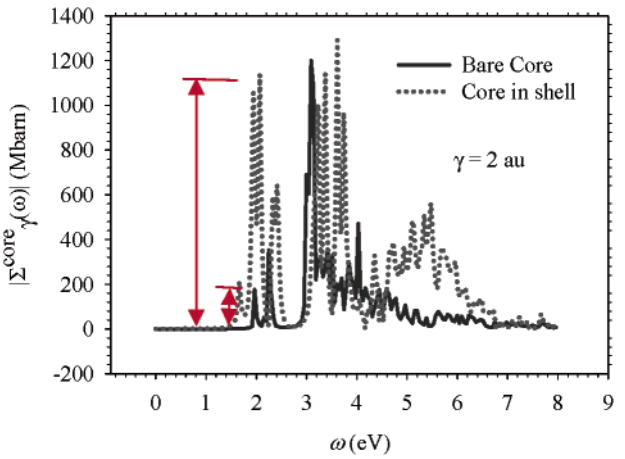

Figure 5. Excitation of the core in the bare and shell-enclosed systems. In most frequency ranges the shell-enclosed core is considerably more active. A pronounced effect appears in several frequency ranges, especially near the plasmon frequency (~2 eV).

Figure 4 shows $\mu_{core}(t)$ for both a bare core (where it is identical to the total dipole moment) and for the enclosed-shell core. It is clear that with the shell, the core has a higher td-dipole moment, which is enhanced by the presence of the shell. A clearer view can be seen in Figure 5, which depicts the function $|\Sigma_\gamma^{core}(\omega)|$, essentially the Fourier transform of the dipole (eq 2.5). The fact that the shell induces a sharp change in the response properties of the core is clear. Indeed, the response of the shell-enclosed core grows by a factor as large as an order of magnitude (as shown by red arrows).

IV. Conclusion and Future Outlook. We showed, using a real-time TDDFT study, that the response of a core system can be profoundly changed when enclosed in a metallic nanoshell. In particular, the core response is greatly enhanced at the shell plasmon-excitation frequency.

Next, it is important to focus on emission. A shell-enhanced emission from the core is of great utility for research in a multitude of fields. Present indications are that similar factors would be found in the emission. Such a calculation will involve a three level paradigm: a 0→2 absorption followed by a 2→1 transition induced by a geometric distortion (nuclear motion) followed by stimulated 0→1 emission. It would further be interesting to study the phenomenon under varying shells, since the one used here has quite larger enhancement factors than may be obtained. Finally, we plan to extend this study to nonsymmetrical arrangements in which a molecule or cluster is in the shell.

Acknowledgment. We acknowledge the support by the National Science Foundation and the Petroleum Research Fund. R.B. gratefully acknowledges support from the German-Israel Fund grant #699. S.W. acknowledges the support of the NIH grant #R01 RR14891-02.

References

(1) West, J. L.; Halas, N. J. *Annu. Rev. Biomed. Eng.* **2003**, *5*, 285.
(2) Fano, U.; Cooper, J. W. *Rev. Mod. Phys.* **1968**, *40*(3), 441.
(3) Pitsillides, C. M.; Joe, E. K.; Wei, X. B.; Anderson, R. R.; Lin, C. P. *Biophys. J.* **2003**, *84*(6), 4023.
(4) Oldenburg, S. J.; Averitt, R. D.; Westcott, S. L.; Halas, N. J. *Chem. Phys. Lett.* **1998**, *288*(2−4), 243.
(5) Prodan, E.; Nordlander, P. *Nano Lett.* **2003**, *3*(4), 543.
(6) Westcott, S. L.; Jackson, J. B.; Radloff, C.; Halas, N. J. *Phys. Rev. B* **2002**, *66*(15).
(7) Prodan, E.; Nordlander, P. *Chem. Phys. Lett.* **2002**, *352*(3−4), 140.
(8) Prodan, E.; Nordlander, P. *Chem. Phys. Lett.* **2001**, *349*(1−2), 153.
(9) Prodan, E.; Nordlander, P.; Halas, N. J. *Chem. Phys. Lett.* **2003**, *368*(1−2), 94.
(10) Perdew, J. P.; Wang, Y. *Phys. Rev. B* **1992**, *45*(23), 13244.
(11) Payne, M. C.; Teter, M. P.; Allan, D. C.; Arias, T. A.; Joannopoulos, J. D. *Rev. Mod. Phys.* **1992**, *64*(4), 1045.
(12) Martyna, G. J.; Tuckerman, M. E. *J. Chem. Phys.* **1999**, *110*(6), 2810.
(13) Baer, R. *Chem. Phys. Lett.* **2002**, *264*, 75.
(14) Baer, R.; Neuhauser, D. *Int. J. Quantum Chem.* **2003**, *91*(3), 524.
(15) Runge, E.; Gross, E. K. U. *Phys. Rev. Lett.* **1984**, *52*, 997.
(16) Kubo, R.; Toda, M.; Hashitsume, N. *Statistical Physics II: Non-equilibrium Statistical Mechanics*, 2nd ed.; Springer-Verlag: Berlin, Heidelberg, 1995.

NL034902K